DOI: 10.2478/cipms-2020-0015

Curr. Issues Pharm. Med. Sci., Vol. 33, No. 2, Pages 76-82

Current Issues in Pharmacy and Medical Sciences

Formerly ANNALES UNIVERSITATIS MARIAE CURIE-SKLODOWSKA, SECTIO DDD, PHARMACIA

journal homepage: http://www.curipms.umlub.pl/

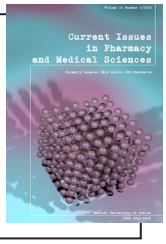

Flow rate effect on partially modified potato starch microspheres formation process

Roaa Mohammed Muneer[1*], Nizar Jawad Hadi[2], Ali Al-Zubiedy[2]

[1] Kerbala Technical Institute, Al-Furat Al-Awsat Technical University, Kerbala, Iraq
[2] Collage of materials engineering, Department of Polymers and Petrochemical industries, University of Babylon, Iraq

ARTICLE INFO

Received 12 August 2019
Accepted 16 September 2019

Keywords:
biopolymer,
starch,
alginate,
glycerol,
rheology,
microfluidic,
microsphere.

ABSTRACT

Natural biopolymers are the most likely choice for biomedical applications, and starches can be considered the best materials for such applications. This comes from the fact of their natural origin and their high biodegradable behavior. Native starches have weak hydrogen bonding and a leaching behavior – making it a candidate for drug delivery application. Still, to make starch useful as a drug delivery carrier, this hydrogen bonding must be strengthened. In this work, native sweet potato starch was used, and the hydrogen bonding between starch molecules was enhanced by introducing glycerol as a hydrogen bonding source and sodium alginate (SA) as a thickener. This blend was tested by means of FTIR and DSC, and based on the test results, improved hydrogen bonding had taken place. Furthermore, potato starch microspheres were successfully produced at different flow rates. In the work, a microfluidic capillary device was harnessed to form microsphere generating total flow rates ranging between (0.00031 and 0.00054) cm^3/sec. Herein, a starch/sodium alginate/glycerol mixture was used as a dispersed phase and PVA+tween 80 was used as continuous phase. At high flow rates (0.00062-0.00054) cm^3/sec, the microspheres took an oval shape. At flow rates (0.00034-0.00048) cm^3/sec, the microspheres took a spherical shape. At very low flow rate (0.00031) cm^3/sec, the microspheres shell was weak and caused core oozing. In this work, starch microspheres were successfully formed with diameter ranging from (151-263) μm.

INTRODUCTION

Two types of difficulties arise when working with biopolymer solutions; the phase diagrams are not universally established and need to be redrawn for any new sample, and immiscibility of synthetic polymers in organic solvents is based on the Flory-Huggins lattice theory (FH) [1]. Polymer microspheres are one of the most common coating types in medicament manufacture and hold several advantages, including encapsulation for many types of drugs such as small molecules, proteins and nucleic acids and are easily administered through a syringe needle [2].

Starches are composed of α-d- glucose with the general chemical composition of (C6H10O5)n and consist of two different polysaccharide molecules (the linear amylose and the highly branched amylopectin). As starch granules are exposed to hot water they swell, lose their crystallinity and leach amylose as they absorb water. As amylose content increases in starch, its swelling ability will decrease, and gel formation will be poor. To improve starch's ability to dissolve in water, chemical and physical modification processing methods produce functional groups that include cross-linked, oxidized, acetylated, hydroxypropylated, partially hydrolyzed molecules. The modification process help strengthen the hydrogen bonding that enhances the ability of starch to form stable gels without leaching [3-5].

Sodium alginate forms hydrogen bonding with water and inter/intra-molecular hydrogen bonding within sodium alginate itself. These bonds break up upon heating, making sodium alginate pass through three states: hydrogen bonded with water → hydrogen bonded with O5 → relatively free, this confirms the existence of inter/intra-molecular hydrogen bonds relating to hydroxyl groups in sodium alginate chains [6]. Besides the strong hydrogen bonding between starch and sodium alginate, low concentrations of glycerol decrease mobility of starch molecules because of the increasing hydrogen bonding that enhances intermolecular interaction [7].

* **Corresponding author**
e-mail: eng.ruaa_89@yahoo.com

Microfluidic flow focusing devices employ two distinct methods of flow control: I. control of the flow rates of two phases and II. control of the inlet pressures of two phases [8]. Flow focusing devices are very popular in microfluidics because they are able to deliver bubbles at frequencies exceeding 105 bubbles per second [9].

The current paper documents the attempt to develop an application to produce natural biopolymer microspheres by way of minimum used of chemical to modify sweet potato starch via the effect of variable flow rate. In the work, flow rate variation was the main generator of shape and size difference of the produced microspheres. To reach this aim, two steps can be justified; the first one was introducing a biopolymer in liquid state made of potato starch without gelation at room temperature, the second was introducing the starch microspheres for biomedical applications with desired shapes and sizes by controlling its rheological properties. A microfluidic glass capillary appliance was used to produce diverse sweet potato starch microspheres via different flow rates.

MATERIALS

Iraqi sweet potato starch, polyvinyl alcohol (PVA) (Mw 1 24 000 Da) – purchased from Sigma Aldrich (New Delhi, India), sodium alginate – purchased from (Central drug house (P) Ltd. New Delhi, India), tween 80 – purchased from (Chemical point, Germany), medical glycerol and deionized water.

Method of microsphere phase preparation

1. Continuous phase

3 g of PVA was dissolved in 100 ml of deionized water using a magnetic stirrer for 1 hour at room temperature, followed by adding 3 ml of Tween 80 with continuous stirring for another 15 minutes. The solution was allowed to stand for 30 minutes before using.

2. Dispersed phase

The dispersed phase consisted of a series of concentrated solutions prepared as follows:

Potato starch was first extracted from Iraqi sweet potato. The potato was granulated and washed with water to allow starch to settle down in the bottom of container. Then the starch was washed 5 times in deionized water and left to settle down so as to decant the water. The resulting starch was then dried in an oven at 50°C for 10 hrs. Subsequently, (1 g) of dried starch was dissolved in deionized water and stirred at 100°C for 15 minutes till the starch become lightly transparent. This was followed by adding (0.25 ml) of glycerol while stirring at 100°C for 20 minutes. This method was applied for each concentration. A sealed glass beaker was then used to hold each diverse sample, the base form of which was developed by adding (1 ml) of ethanol to the solution and stirring for 15 minutes. The samples were then cooled to room temperature and left for 5 days before using.

To enhance starch flow properties and to raise its viscosity so as to be able to flow from a microfluidic device, sodium alginate was added to the diverse solutions from the beginning of processing. Alginate was used as thickening material because of its ability to increase the viscosity of starch at low concentration [10].

In doing so, 1 gram of processed potato starch was mixed with (0.5 g) of sodium alginate and added slowly to cold water with stirring to prevent alginate crumpling. The temperature of solution was then raised to 100°C while being continuously stirred for 30 minutes; the process taking place in a sealed glass beaker. After 20 minutes, (0.25 ml) of glycerol was added with stirring continued, while at 100°C for another 20 minutes. Subsequently, (1 ml) of ethanol was added to the solution with continuous stirring for another 15 minutes. Caution must be taken in this step because of the high evaporation rate of water in the sealed beaker to avoid losing the solution through boiling. The resulted solution was cooled and left 5 days before using.

Microfluidic system

This part of work includes assembling the microfluidic system. This system consists of two units; *the microfluidic capillary*; *the syringe pumps*. The main part of this system is the *microfluidic capillary* in which the rheology of the biopolymer was studied experimentally. The micro capillary was formed from glass micro capillary tube of L shape that contains a flow focusing regime chamber. The dimensions of the micro capillary is (60 mm of 300 µm inner diameter × 36 mm of 400 µm inner diameter) with flow focusing chamber of (4 mm × 6 mm). The capillary geometry and dimension is as Sin *et al.,* [11] used, with slight modification in microfluidic capillary geometry. The device is revealed in Figure 1.

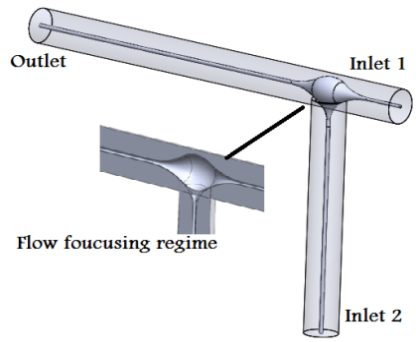

Figure 1. A scheme illustrating the micro capillary flow focusing regime

Two syringe pumps were used, one is connected by Teflon tubing to inlet 1 (disperse phase) and the other was connected (by Teflon tubing) to inlet 2 (continuous phase). The outlet was connected by Teflon tubing to the collecting beaker containing the (PVA + tween80) solution as collecting phase. Medical rubber sealing was used to fix the needles, (32 gauge) for the dispersed phase and (27 gauge) for the continuous phase, and prevent their moving. The full device is revealed in Figure 2.

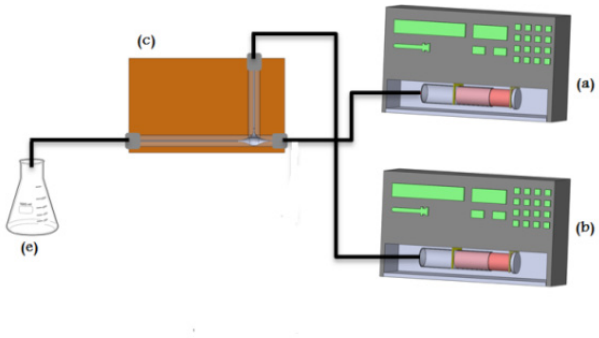

Figure 2. A scheme of a Microfluidic system: (a) syringe pump to deliver disperse phase, (b) syringe pump to deliver continuous phase, (c) micro capillary, (e) collecting beaker

Characterization

1. **Fourier-transform infrared spectroscopy FTIR.** This test was used to investigate the starch interaction with different compounds. Instrumentation was supplied by Shimadzu Scientific, USA
2. **Differential scanning calorimetry DSC.** DSC was applied to study the thermal degradation of microspheres (DSC-60, Shimadzu Scientific, USA).
3. **Cone plate viscometer.** This test was employed to examine viscosity and shear stress coefficient functions as functions of shear rate and temperature (Brookfield DV III ultra-programmable rheometer, Centre for Industrial Rheology, UK).
4. **Optical microscope.** The microsphere morphology was investigated by means of an optical microscope using wet mode, where the microspheres were floating in continuous phase.

RESULTS AND DISCUSSION

1. Fourier-transform infrared spectroscopy results

The potato starch functional groups were confirmed by comparison to reference starch FTIR spectra. The bands were almost similar (Figure 3). [12].

Figure (4) shows the FTIR spectrum for pure potato starch at several concentrations. The spectrum showed a sharp band at different wavelengths 3379-3387 cm^{-1}, indicating the presence of a strong OH group [13]. This is a result of the existence of hydrogen bonding interaction with starch molecules [7]. This hydrogen bonding came from the supplied glycerol which contains three hydrophilic alcoholic hydroxyl groups that affect its water solubility and hygroscopic nature [14]. Another band is seen at 1049-1059 cm^{-1} and indicates C-O stretching within the -C-O-C-. -C-OH groups (Figure 4) [12]

By adding alginate to solution, in comparison to pure starch and plasticized starch, another sharp band appeared around 1612 cm^{-1}. This is indicative of carboxylate anions producing strong stretching vibrations. Such effect is evidence of interaction between sodium alginate and potato starch (Figure 5) [15].

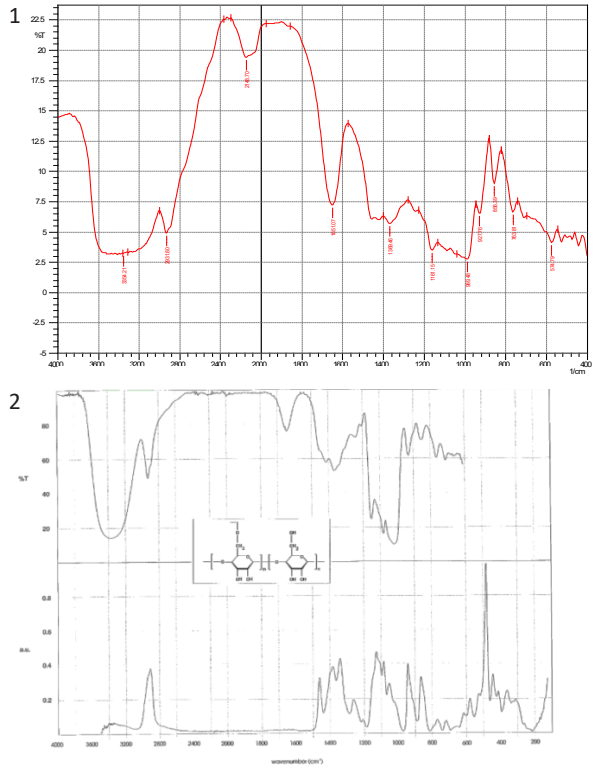

Figure 3. FTIR spectrum for: (1) pure potato starch; (2) starch reference

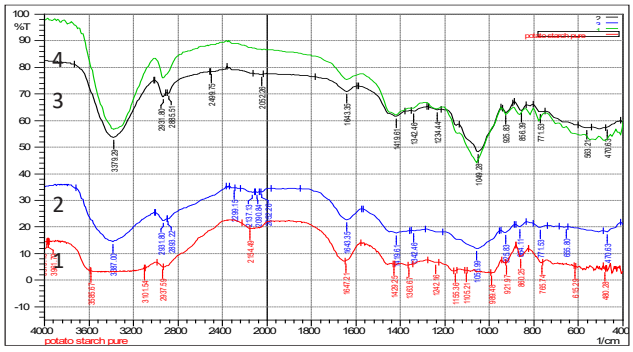

Figure 4. FTIR spectrum for: (1) pure potato starch; (2) 1 g potato starch + 0.25 ml glycerol; (3) 1.5 g potato starch + 0.50 ml glycerol; (4) 2 g potato starch + 0.75 ml glycerol

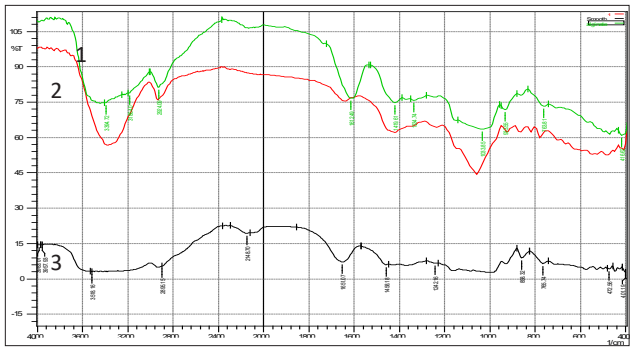

Figure 5. The FTIR spectrum of: (1) Sodium alginate; (2) plasticized potato starch; (3) pure potato starch

2. Differential scanning calorimetry DSC results

This test was used to investigate the interaction between starch and glycerol in forming partially modified starch. The glass transition temperature T_g revealed an increase

of temperature from 50.29°C for native starch, to 66.01°C for partially modified starch and to (69.72°C) for the sodium alginate/starch solution. This increase in T_g is an indicator of the presence of the hydrogen bonding between starch molecules. It should be noted that these need external energy to move to glass transition and overcome the intermolecular interactions causing high T_g (Figure 6-8).

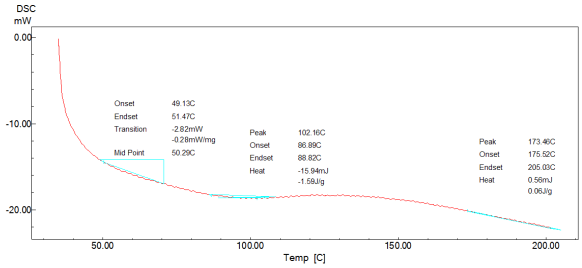

Figure 6. DSC diagram for pure potato starch

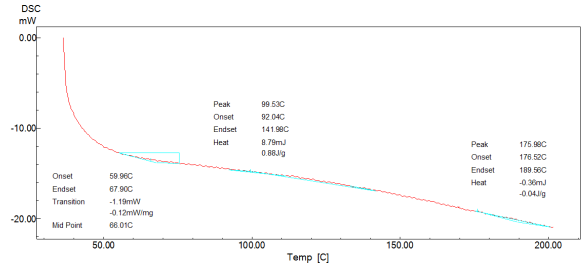

Figure 7. DSC diagram for potato starch/glycerol

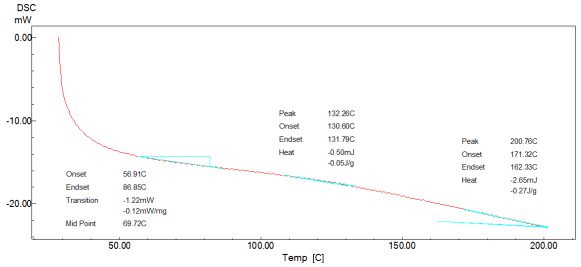

Figure 8. DSC diagram for potato starch/glycerol/sodium alginate

3. Cone plate viscometer results

3.1. Continuous phase

Prediction of flow rates for both dispersed and continuous phases were done rheologically using a cone plate viscometer with CPA – 42 Z spindle [16]. It can be seen in Figure 9 that viscosity decreased with shear rate increase. This effect reveals syringe pump flow rates (Figure 9).

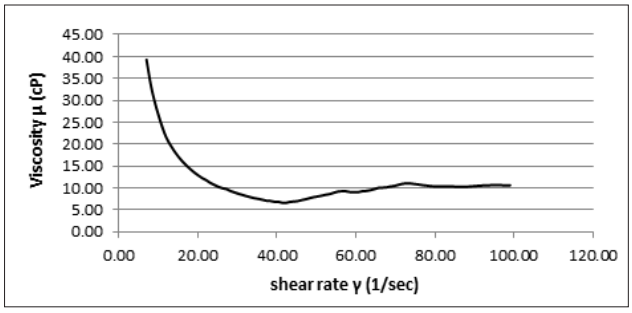

Figure 9. The behavior of viscosity versus shear rate at Log scale with increasing spindle speed

3.2. Dispersed phase

Since potato starch was naturally extracted, its behavior was not clear or justified. To qualify the behavior of potato starch, three concentrations of pure potato starch as used in this experiment were evaluated using a cone plate viscometer (Table 1).

Table 1. Viscosity of potato starch at different concentrations

Concentration %	Temperature °C	Viscosity (cP)
1	20	7.05
1.5	20	12.09
2	20	24.78

The viscosity was found to increase with increased concentration. This is the standard behavior of starch. By plotting viscosity versus shear rate, as seen in Figure 10, the behavior exhibited shear thinning; the viscosity decreased as shear rate increased.

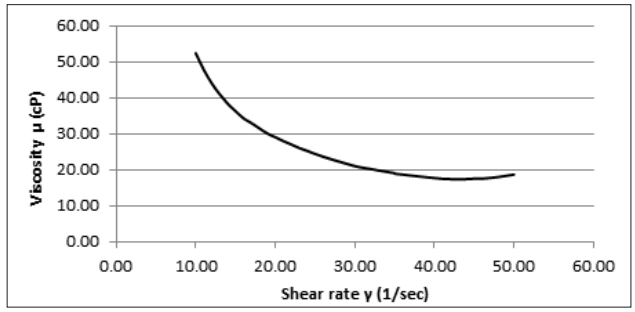

Figure 10. Shear rate versus viscosity behavior for potato starch

Adding sodium alginate as a thickening phase to potato starch sharply increased the viscosity of this solution, as compared to basic (potato starch + glycerol) solution. The viscosity/shear rate behavior still demonstrated shear thinning, where viscosity decreased with increased shear rate (Figure 11).

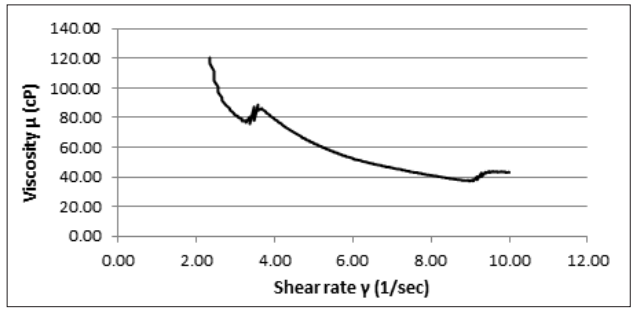

Figure 11. Shear rate versus viscosity behavior for potato starch and sodium alginate

4. Break up phenomenon

Since potato starch flow through the microfluidic device met with difficulty, alginate was used as thickening material because of its ability to increase the viscosity of starch at low concentration [10]. This ability induces the potato starch to form oval to spherical shapes at different flow rates (Figure 12). Sodium alginate forms strong hydrogen bonding due to heating, by the formation of inter/intramolecular hydrogen bonding within its chains, for example, $O^3H^3\ldots O^5$ and $O^2H^2\ldots O{=}C{-}O{-}$ [6].

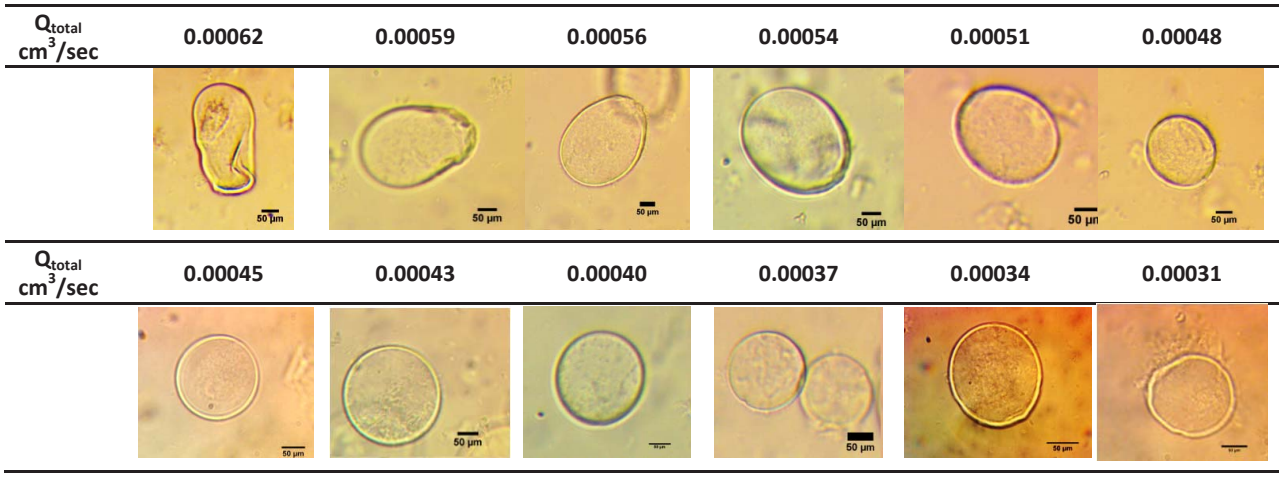

Figure 12. Optical microscope images at different flow rates

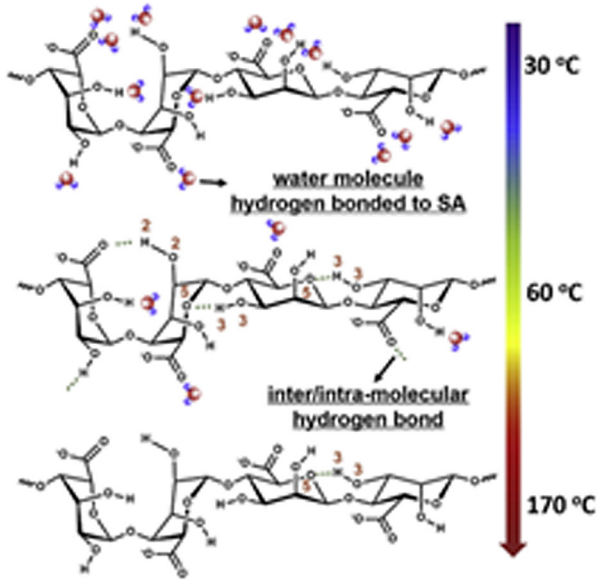

Figure 13. Schematic of the heat-induced hydrogen bonding transformation in sodium alginate [7]

As shown in Figure 13, sodium alginate forms hydrogen bonding with water and inter/intra-molecular hydrogen bonding within sodium alginate itself. These bonds are broken up upon heating, making sodium alginate pass through three states: hydrogen bonded with water → hydrogen bonded with O_5 → relatively free. This confirms the existence of inter/intra-molecular hydrogen bonds relating to hydroxyl groups in sodium alginate chains [6].

Besides the strong hydrogen bonding between starch and sodium alginate, low concentrations of glycerol decrease the mobility of starch molecules because of increasing hydrogen bonding that enhances intermolecular interaction [7]. Multiphase flow creates two flow rates; Q_c for continuous phase and Q_d for dispersed phase. The total flow rate can be calculated using equation (1) [17].

$$V = \frac{Q_{total}}{A} = \frac{Q_c + Q_d}{A} \quad (1)$$

The flow of a fluid through a microfluidic channel can be characterized by its Reynolds number. The Reynolds number for a microfluidic device can be defined as the following:

$$Re = \frac{(\rho\, U\, a)}{\mu} \quad (2)$$

Where ρ is continuous phase density, U is sphere velocity, a is the sphere radius flow through microchannel and is liquid viscosity [18].

$$U = \frac{Q_{total}}{\pi a^2} \quad (3)$$

The characteristic velocity of the flow is the relation between flow rate divided by capillary area [19]. When the Reynolds number is less than 10^2, the flow can be considered laminar [20]. When the Reynolds number versus flow rate is plotted, this shows that the given Reynolds numbers is proportional to increased flow rate, with value less than one leading to laminar flow [21] chemical synthesis and biochemical assays. Within this platform, the formation and merging of droplets inside an immiscible carrier fluid are two key procedures: (i (Figure 14).

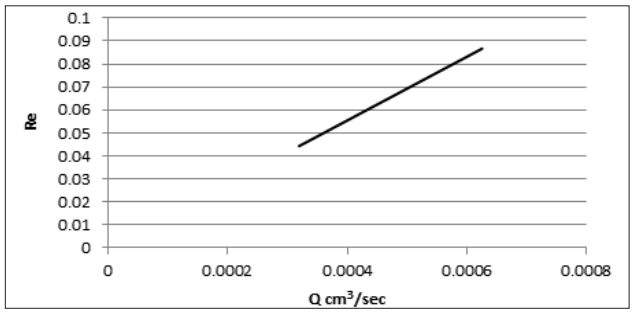

Figure 14. Reynolds number versus flow rates.

The total microsphere diameter was plotted against flow rate (Figure 16). Herein, it is evident that the microsphere diameter first decreased with increased flow rate and then increases; this point is called the critical flow rate. This means that flow rate less than 0.00048 cm/sec has microsphere diameter from (151-180) µm, and this range rises to between (195-263) µm at higher flow rate. At very low flow rate (0.00031 cm^3/sec), the microsphere shell becomes weak and breaks, voiding the core. This behavior indicates that the shear rate was not high enough to enable the shell to have uniform shape (Figure 15).

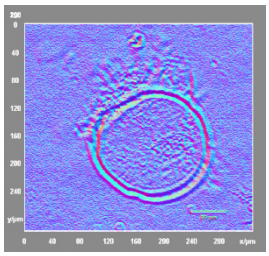

Figure 15. Weak shell formation due to low flow rate (0.00031 cm^3/sec)

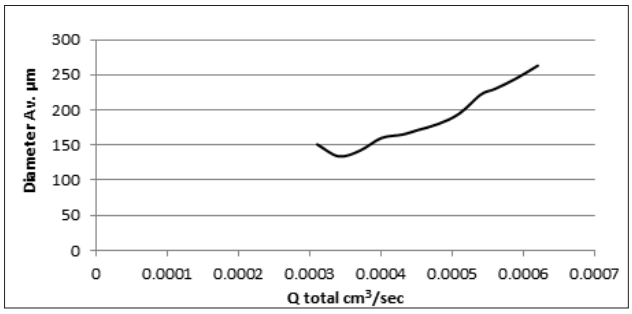

Figure 16. Flow rates versus average diameter of microspheres

The shape of microsphere was much related to flow rate, where the microspheres shape ranged from oval to complete sphere with varying flow rates (Figure 15). At high flow rate (0.00062-0.0051 cm^3/sec) the microspheres did not take on a spherical shape, forming an elongated oval shape instead (Figure 17).

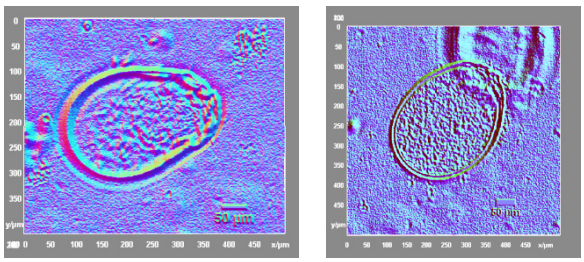

Figure 17. Microspheres deformation at high flow rates, (a) 0.00059 cm^3/sec; (b) 0.00056 cm^3/sec

This deformation in shape comes from the high hydrodynamic forces that overcome the interfacial tension of the microsphere and change its shape or even induce breakup (Figure 18) [22].

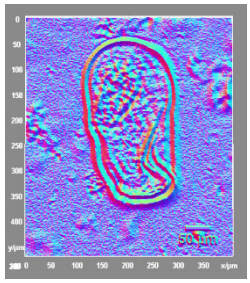

Figure 18. Microsphere breakup at high flow rate 0.00062 cm^3/sec

At low viscosity, the microsphere tends to return to a spherical radius by the effect of interfacial tension of the microsphere core, in conjunction with slowing down of motion within the continuous phase. At higher viscosities, shape change is produced by the microsphere not having enough time to fully developed as spheres (Figure 19) [22].

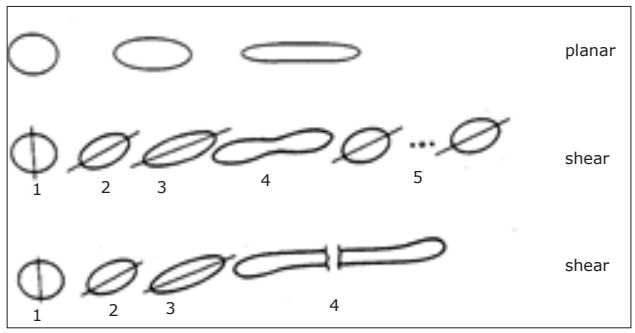

Figure 19. The influence of deformation rate, type of flow, and viscosity ratio on the deformation of droplets in shear and extensional flow. At high deformation rates (right-hand shapes), drop breakup can occur. Adapted from Rumscheidt and Mason (1961)

CONCLUSION

Strengthening starch molecular structure by enhancing hydrogen bonding will make starch more acceptable for microsphere formation when using microfluidic devices. In our work, we found that flow rate was the controlling parameter of microsphere shape and morphology. Low starch concentrations with the addition of sodium alginate modified the viscosity at this concentration. At high flow rates, (0.00062-0.00054) cm^3/sec, microspheres deform and shift up from spherical to oval shapes. By decreasing flow rates, (0.00048-0.00034 cm^3/sec), the microsphere starts to have a spherical shape. However, at too low flow rates (0.00031 cm^3/sec), the spheres do not fully form.

ACKNOWLEDGEMENTS

This work was supported by training and financial assistance provided by the college of materials engineering, department of polymers and petrochemical industries, University of Babylon, Iraq.

ORCID iDs

Roaa Mohammed Muneer https://orcid.org/0000-0003-4220-6202
Nizar Jawad Hadi https://orcid.org/0000-0003-2665-2608
Ali AL-Zubiedy https://orcid.org/0000-0002-2041-2737

REFERENCES

1. Costeux A. Water in water emulsions : phase separation and rheology of biopolymer solutions. *Rheol Acta*. 2001;40;441-56.
2. Kim KK, Pack DW. Microspheres for Drug Delivery. *BioMEMS Biomed Nanotechnol*. 2006:19-50.
3. Parker R, Ring SG. Aspects of the physical chemistry of starch. *J Cereal Sci*. 2001;34:1-17.
4. Singh N, Singh J, Kaur L, Sodhi NS, Gill BS. Morphological, thermal and rheological properties of starches from different botanical sources. *Food Chem*. 2003;81(2):219-31.
5. Li J, Yeh A Relationships between thermal, rheological characteristics and swelling power for various starches. *J Food Eng*. 2002;50(3):141-8
6. Hou L, Wu P. Exploring the hydrogen-bond structures in sodium alginate through two- dimensional correlation infrared spectroscopy. *Carbohyd. Polym*. 2019;205:420-6.

7. Liang J, Ludescher RD. Effects of glycerol on the molecular mobility and hydrogen bond network in starch matrix. *Carbohyd Polym*. 2015;115:401-7.
8. Ward T, Faivre M, Abkarian M, Stone HA. Microfluidic flow focusing: Drop size and scaling in pressure versus flow-rate-driven pumping. *Electrophoresis*. 2005;26(19):23716-24.
9. Garstecki P, Gitlin I, Diluzio W, Whitesides GM, Kumacheva E, Stone HA. Formation of monodisperse bubbles in a microfluidic flow-focusing device. *Appl Phys Lett*. 2004;85(13):2649-51.
10. Hou L, Wu P. Exploring the hydrogen-bond structures in sodium alginate through two- dimensional correlation infrared spectroscopy. *Carbohydr Polym*. 2019;205:420-6.
11. Ward T, Faivre M, Abkarian M, Stone HA. Microfluidic flow focusing: Drop size and scaling in pressure versus flow-rate-driven pumping. *Electrophoresis*. 2005;19(26):3716-24.
12. Kuptsov AH, Zhizhin GN. *Handbook of fourier transform raman and infrared spectra of polymers*; 1998.
13. Sarifuddin NASN, Zaki HHM, Azhar AZA. The effect of glycerol addition to the mechanical properties of the thermoplastic films based on jackfruit seed starech. *Malaysian J Anal Sci*. 2018;22(5):5:892-8.
14. Pagliaro BM, Rossi M, Pagliaro M. Glycerol: Properties and Production In: *The Future of Glycerol: New Uses of a Versatile Raw Material*; 2008:1-18.
15. Taha MO, Aiedeh KM, Al-hiari Y, Alkhatib HS. Synthesis of zinc-crosslinked thiolated alginic acid beads and their in vitro evaluation as potential enteric delivery system with folic acid as model drug. *Pharmazie*. 2005:60.
16. Labs BE. *More solutions to sticky problems* (A guide to getting more from your Brookfield Viscometer and Rheometer); 2014.
17. Adzima BK, Velankar SS. Pressure drops for droplet flows in microfluidic channels. *J Micromech Microeng*. 2006;16(8):1504-10.
18. Ham D, Lee H, Westervelt RM. Introduction to fluid dynamics for microfluidic flows. In: *CMOS Biotechnology*. Springer Ltd; 2007:5-30.
19. Holmes DP. *Confined fluid flow: Microfluidics and capillarity*. Uni Roma; 2015.
20. Slapar V. *Microfluidics*. University of Ljubljana; 2008.
21. Gu H, Duits MHG, Mugele F. Droplets formation and merging in two-phase flow microfluidics. *Int Mol Sci*. 2011;12(4) 2572-97.
22. Macosko CW. *Rheology: Principles, Measurements and Applications*. Wiley-VCH, Inc; 1994.